

k -space formulation of Γ - X mixing for excitons in a thin GaAs/AlAs quantum well

C. P. Chang and Yan-Ten Lu

Department of Physics, National Cheng Kung University, Tainan, Taiwan

(Received 15 September 1993)

Using a nonvariational method in k space, we study the effects of Γ - X valley mixing on the structure of excitons in an asymmetric $\text{Al}_x\text{Ga}_{1-x}\text{As}/\text{AlAs}/\text{GaAs}/\text{Al}_x\text{Ga}_{1-x}\text{As}$ quantum well. The formulation of excitons in this system involves two complications due to Γ - X mixing: the nonparabolic subband structures in the xy plane, and the Coulomb interaction between different electronic subbands. These effects lead to a set of two coupled integral equations. The eigenvalues and functions thus obtained are then used to compute the optical absorption spectra for various structures near the Γ - X crossing.

I. INTRODUCTION

The band-edge diagram of the structure $\text{Al}_{0.5}\text{Ga}_{0.5}\text{As}/\text{AlAs}/\text{GaAs}/\text{Al}_{0.5}\text{Ga}_{0.5}\text{As}$ possesses a Γ well in the GaAs layer and an X well in the AlAs layer, as shown in Fig. 1. When the width of GaAs is less than 30 Å, the confinement effect lifts the energies of the Γ levels higher than the bottom of the X well. The lowest electronic state is formed either by a Γ electron (type I) or by an X electron (type II). For a type-II structure, electrons and holes are separated in real space and k space, which leads to low optical efficiency, long recombination-time constant, and characteristic low-power optical nonlinearity.^{1,2} However, the type-I structure shows substantially different properties. The crossover from type I to type II has been observed experimentally by changing the layer width,³⁻⁹ and by applying an electrical field^{1,10-12} or hydrostatic pressure.¹³⁻¹⁵ Recently, more attention has been given to such structures,¹⁶⁻²⁷ following the observation of their vast potential for devices such as electrically tunable light sources, optical switching, and optical computing.

In a quantum well, the excitonic effect is enhanced by the spatial confinement and therefore dominates many

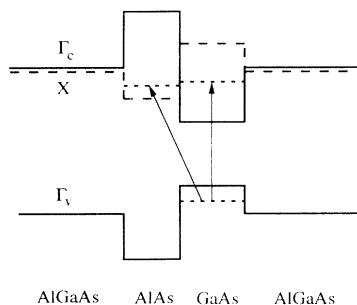


FIG. 1. Band-edge diagram of $\text{Al}_{0.5}\text{Ga}_{0.5}\text{As}/\text{AlAs}/\text{GaAs}/\text{Al}_{0.5}\text{Ga}_{0.5}\text{As}$ quantum well. The solid lines depict the staggered band edges at the Γ point for both valence bands Γ_v and conduction bands Γ_c . The dashed lines show the edges of the X conduction bands. The energy of the lowest confined level in each valley is indicated by the short-dashed lines, and the transition energies are shown by the arrowed lines.

linear and nonlinear optical properties even at room temperature. For simply type-I or type-II structures, there have only recently been realistic calculations of the excitonic structures.²⁸⁻³³ Most of them are based on variational methods. Nonvariational methods have been developed most recently for the type-I structures, in which the exciton wave functions are expanded in terms of the subband envelope functions.^{28,34-36} This multiple-band expansion leads to a set of n coupled differential equations if the lowest n subbands are included in the expansion. The numerical complications make the practice in real space almost unfeasible even for n as small as 2.³⁴ On the other hand, the formulation in k space has been proved successful in exactly or quasi-two-dimensional systems, and yields solutions comparable with the analytical solutions in the exactly two-dimensional system if one uses a selected Gaussian quadrature method.³⁵⁻³⁶ In this work, we will extend the k -space formulation to include the effect of Γ - X mixing.

In a heterostructure, the interface breaks the symmetrical properties of the bulk semiconductor and couples different Bloch states. Consequently, the levels in the X_z valley are coupled to the levels in the Γ valley.¹⁶ The mixing is strongly enhanced when a confined X level is close in energy to a Γ level, which affects the formulation for the exciton in the following two ways: (1) the subband structures in the xy plane become nonparabolic, as shown in Fig. 2, and (2) this system possesses two nearly degenerate levels centered at different layers. Consequently, besides the hole component, the electronic part of an exciton wave function should contain at least two states. These two states are coupled by the intervalley mixing and their Coulomb interactions with holes (multiband effect). In a recent report, Aleiner *et al.*⁹ presented a calculation of exciton energies for quantum wells near the Γ - X crossing. With a variational method, they first computed the $1s$ excitonic state for each of the two bands, and then coupled these two $1s$ states through the valley mixing potential. This procedure excluded the multiband Coulomb interaction. Moreover, near the Γ - X crossing the effect of valley mixing is comparable with the excitonic effect, and therefore it is better to treat both effects equally. In this work, we will present a nonvariational method in k space, which takes equally into considera-

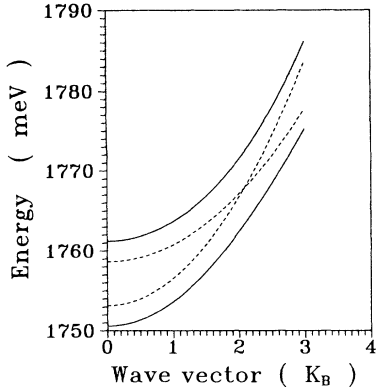


FIG. 2. In-plane band structure for AlAs(25 Å)/GaAs(31 Å). The dashed curves are the subband structures of Γ and X valleys without valley mixing. The Γ band possesses a smaller effective mass. The solid curves show the band structures with valley mixing.

tion both the valley mixing and the multiband Coulomb interaction. After solving the eigenvalues and envelope functions for excitons, we then compute the optical absorption spectra for structures near the level crossing.

II. FORMULATION OF THE EXCITON WITH Γ - X VALLEY MIXING

A. Model of Γ - X valley mixing

In a bulk semiconductor, a Γ state and an X state are mutually independent. In a heterostructure, the periodicity in the z direction is terminated at the interface. The termination of the periodic structure couples states in the Γ valley and the X_z valley. Since the effects of valley mixing can only be appreciated when a Γ level is close in energy to an X level, one can write the mixed electron wave function as a linear combination of these two levels:

$$\Psi_{\mathbf{K}}(\mathbf{r}) = a\Psi_{\mathbf{K}}^{\Gamma}(\mathbf{r}) + b\Psi_{\mathbf{K}}^X(\mathbf{r}), \quad (1)$$

where $\Psi_{\mathbf{K}}^{\Gamma}(\mathbf{r})$ and $\Psi_{\mathbf{K}}^X(\mathbf{r})$ are the wave functions of the Γ and X electrons, with an in-plane wave vector \mathbf{K} . Each function satisfies the Schrödinger equation:

$$\left\{ \frac{-\hbar^2 \nabla^2}{2m_i^*} + V_i(z) \right\} \Psi_{\mathbf{K}}^i(\mathbf{r}) = E_{\mathbf{K}}^i \Psi_{\mathbf{K}}^i(\mathbf{r}); \quad (2)$$

where m_i^* is the effective mass of valley i and the index i denotes Γ or X . $V_i(z)$ is the staggered potential of the i valley, as shown in Fig. 1. As for the valley mixing, we adopt a delta potential, V_{mix} , at the interfaces to couple these two states. This potential was previously introduced by Liu to calculate the tunneling current for a GaAs/AlAs quantum well,³⁷ and used by several authors in solving the valley-mixing problem.^{1,33}

$$V_{\text{mix}} = \sum_i \beta \delta(z - z_i) (|\Gamma\rangle\langle X| + |X\rangle\langle \Gamma|), \quad (3)$$

where the parameter β gives the strength of valley mixing caused by an interface at z_i . Within the two-band expansion in Eq. (1), the Hamiltonian becomes a 2×2 matrix

$$\begin{bmatrix} H_{\Gamma} & V_{\text{mix}} \\ V_{\text{mix}} & H_X \end{bmatrix}, \quad (4)$$

where H_{Γ} and H_X are the Hamiltonians given in Eq. (2). Figure 3 plots the transition energies (from the valence level to the conduction level) as functions of the thickness of the GaAs layer with AlAs fixed at 25 Å. These two bands cross when the GaAs is 30-Å thick. We estimate β to be $-0.46 \text{ meV } \text{Å}$ which yields about a 10-meV splitting near the level crossing in agreement with experimental observations.^{1,11} The in-plane band structures of a quantum well with 25-Å AlAs and 31-Å GaAs are depicted in Fig. 2. Valley mixing causes an anticrossing near the intersection, and therefore the resultant subbands are nonparabolic.

B. Exciton equation in k space

Now, we will add to the formulation the screened Coulomb interaction between an electron at \mathbf{r}_e and a hole at \mathbf{r}_h ,

$$V_c = -\frac{e^2}{\epsilon|\mathbf{r}_e - \mathbf{r}_h|}. \quad (5)$$

To avoid the complications arising from different dielectric layers,^{38,39} we assume a dielectric constant 12.4 for both AlAs and GaAs. A static exciton wave function is expanded as linear combinations of the subbands of electrons and holes:

$$\Phi(\mathbf{r}_e, \mathbf{r}_h) = \sum_{n,m,i} \phi_{n,m}^i(\mathbf{K}) f_n^i(z_e) g_m(z_h) \times e^{i\mathbf{K} \cdot (\mathbf{R}_e - \mathbf{R}_h)} \mu_c^i(\mathbf{r}_e) \mu_h(\mathbf{r}_h), \quad (6)$$

where i stands for the band index, Γ or X ; and f_n and g_m denote the envelope functions. The indices n and m sum over the confined levels. \mathbf{K} and \mathbf{R} are the in-plane momentum and position vectors. The function μ is the periodic part of the Bloch state for each band. If the lowest N_X , N_{Γ} , and M_h levels of the corresponding valley

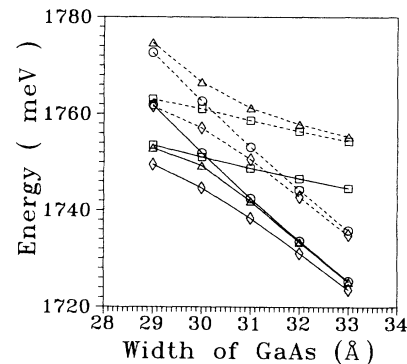


FIG. 3. Transition energies (from a valence to a conduction level) as functions of the GaAs width. Solid and dashed lines indicate the results with or without excitonic effect, respectively. Among the dashed lines, \square (\circ) shows the level of Γ (X) without valley mixing, and \diamond and \triangle indicate the levels with valley mixing. Among the solid lines, \square (\circ) indicates the one-band exciton level of Γ (X), \triangle the lowest level with multiband effect but without valley mixing, and the \diamond symbols the level with both effects.

are included in the expansion, the Hamiltonian is then converted into a set of $(N_X + N_\Gamma) \times M_h$ coupled differential equations. These coupled equations yield the exciton energies and the corresponding envelope functions $\phi_{n,m}^i$. The numerical process of solving these coupled equations is easier in k space than in real space. The transformation to the momentum space is in principle the same as that in the quasi-two-dimensional (2D) system, which has been given in Ref. 35. Consequently, an envelope function $\phi_{n,m}^i$ couples to another $\phi_{n',m'}^i$ through the following quasi-2d Coulomb interaction in k space:

$$V_{n,m,i}^{n',m',i'}(\mathbf{K}-\mathbf{K}') = \frac{-e^2}{2\pi\epsilon|\mathbf{K}-\mathbf{K}'|} \times \int \int dz_e dz_h e^{-|\mathbf{K}-\mathbf{K}'||z_e-z_h|} \times f_n^i(z_e) f_{n'}^{i'}(z_e) g_m(z_h) g_{m'}(z_h), \quad (7)$$

$$\begin{bmatrix} E_X(\mathbf{K}) - E_h(\mathbf{K}) & \beta f^\Gamma(z_i) f^X(z_i) \\ \beta f^\Gamma(z_i) f^X(z_i) & E_\Gamma(\mathbf{K}) - E_h(\mathbf{K}) \end{bmatrix} \begin{bmatrix} \phi_X(\mathbf{K}) \\ \phi_\Gamma(\mathbf{K}) \end{bmatrix} + \sum_{\mathbf{K}'} \begin{bmatrix} V_X^X(\mathbf{K}-\mathbf{K}') & V_X^\Gamma(\mathbf{K}-\mathbf{K}') \\ V_\Gamma^X(\mathbf{K}-\mathbf{K}') & V_\Gamma^\Gamma(\mathbf{K}-\mathbf{K}') \end{bmatrix} \begin{bmatrix} \phi_X(\mathbf{K}') \\ \phi_\Gamma(\mathbf{K}') \end{bmatrix} = E \begin{bmatrix} \phi_X(\mathbf{K}) \\ \phi_\Gamma(\mathbf{K}) \end{bmatrix}, \quad (8)$$

where E_X , E_Γ , and E_h are the band energies of X , Γ , and heavy-hole bands. The valley mixing couples Γ levels and X levels of the same in-plane wave vector \mathbf{K} , since the valley-mixing potential preserves the translational symmetry in the xy plane, whereas the multiple-band Coulomb interaction breaks this symmetry and couples all \mathbf{K} states. We use 200 Gaussian points to carry out the integration over \mathbf{K}' . The details of the numerical treatment have been discussed in Ref. 36. After obtained the eigenvalues and eigenfunctions, we then compute the absorption spectrum. The expression of the absorption coefficient in k space is readily given in Ref. 35. Within a constant factor, the absorption coefficient α can be written as:

$$\alpha(\omega) \propto \sum_n \frac{\Gamma_w}{(E_n - \hbar\omega)^2 + \Gamma_w^2} \times \left| \sum_{\mathbf{K}} \langle f^X | g \rangle \phi_{nX}(\mathbf{K}) + \langle f^\Gamma | g \rangle \phi_{n\Gamma}(\mathbf{K}) \right|^2, \quad (9)$$

where E_n is the n th eigenvalue of Eq. (8), and Γ_w is the Lorentzian broadening parameter, set equal to 1.5 meV in this work. This value smoothes the sharp absorption spectrum while still keeping the transition peaks of interest distinguishable. In Eq. (9), the overlap integral between the X level and the heavy-hole level, $\langle f^X | g \rangle$, is in practice negligible due to the spatial separation.

III. RESULTS AND DISCUSSION

For comparison, we first switch off the potentials of valley mixing and multiple-band Coulomb interaction in Eq. (8). This allows us to calculate the one-band exciton binding energies for Γ and X subbands separately. In Fig. 3, we plot the resultant energies of the lowest exciton

where the $f_n(g_m)$ is the envelope function of the n th (m th) conduction (valence) subband.

For the structures under study, about 25-Å AlAs and 30-Å GaAs, each of the X and Γ wells contains only a confined level. The energies of these two levels are nearly degenerate. (For levels with large energy separation, the two mixing mechanisms, valley mixing and multiband Coulomb interaction, are both negligible.) In order to concentrate on the effect of Γ - X mixing, we will simplify the structure of the holes. Only the lowest heavy-hole subband is included. The interference between light hole and heavy hole is neglected. This simplification does not affect the characteristic features of Γ - X mixing. Hereafter, we will omit the subscripts n and m . Under these conditions, we obtain a set of two coupled convoluted equations for s -wave excitons:

levels (solid lines) against the GaAs width with AlAs fixed at 25 Å. The one-band exciton binding shifts each subband to a lower energy. A crossing of these two $1s$ levels occurs when the width of GaAs equals 30.2 Å. The exciton binding energies are 10.7 and 10.1 meV for Γ and X when the GaAs is 30-Å wide, and drop to 10.2 and 9.2 meV when the GaAs width is increased to 40 Å. Exciton binding energies for both valleys decrease as the GaAs layer grows thicker. This trend is consistent with other reports.³⁰⁻³³

We then switch on the multiple-band Coulomb interaction. The energies of the lowest exciton level are also shown in Fig. 3. This coupling slightly pushes down the lower $1s$ level between Γ and X valleys. For the 25/30 (AlAs/GaAs) structure, the lowest exciton level is AlAs- X -like, and becomes GaAs- Γ -like for the 25/31 structure. The shift is appreciable only near the crossing point. The maximum energy shift at the crossing point is about 2 meV. The $1s$ level of the higher subband is now embedded in the continuum of the lower subband for most structures except 25/29 and 25/30, and becomes a Fano-like resonance.⁴⁰ The interference between heavy hole and light hole exhibits a similar phenomenon.²⁸ The difference is that the wave functions of the resonance and the continuum are both in the same layer for the case of holes, but they are separated in different layers in the case of Γ - X mixing.

In Fig. 4, the dashed curves depict the computed absorption spectra for structures from 25/29 to 25/33. For 25/29, the X $1s$ level causes a small bump at the lower-energy side of the Γ $1s$ peak. This transition is due to the multiband Coulomb interaction. We can also identify the Γ $2s$ peak because of the small value of Γ_w . For 25/30, two peaks of nearly equal intensity indicate strong mixing between the two $1s$ states. The level crossing occurs between 25/30 and 25/31. For structure 25/31, the X $1s$

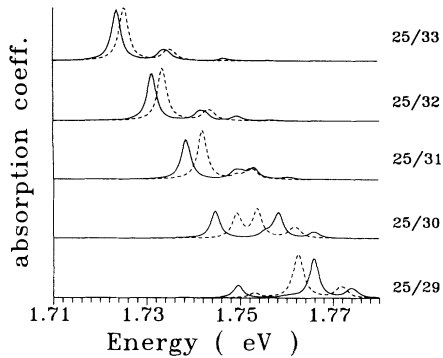


FIG. 4. Absorption coefficients for various quantum wells. The dashed curves show the computed absorption coefficients with the multiband effect but without the valley-mixing effect. The solid curves are the results with both effects. The numbers indicate the widths of AlAs/GaAs for each curve.

state is close to the Γ 2s, and appears like a shoulder of the 2s peak. For 25/32 and 25/33, the coupling between X and Γ becomes so weak that the X 1s peak is no longer visible.

We now switch on the valley-mixing potential, V_{mix} . It further lowers the lowest excitonic state as shown in Fig. 3. Within the range of our study, the effect of valley mixing is apparently much stronger than that of the multiple-band Coulomb interaction. The absorption

spectra are also shown in Fig. 4 as solid curves. Valley mixing increases the peak intensities of X 1s levels. For 25/33 and 25/32, the X levels become visible. In the spectrum of 25/31, the X level is now distinguishable from the Γ 2s level. Valley mixing also pushes apart two closed levels. This can be seen clearly in the spectrum of 25/30, where two originally nearly degenerate levels are now separated by 14 meV and exhibit equal peak intensity. For structures 25/29 and 25/30, the X 2s levels appear as shoulders on the Γ 1s peaks.

When the GaAs width is increased from 29 to 31 Å, the lowest exciton level changes from AlAs-X-like to GaAs- Γ -like, and the absorption coefficient of the lowest level is increased by a factor 3. This factor grows to 10, if we compare two structures like 25/27 and 25/33 which are not so close to the crossing point. This is comparable with the experimental observation.¹ In experiment, the crossing of levels is achieved by applying an external electrical field, instead of varying the layer thickness. Our formulation in k space can include the Stark effect with little modification. We intend to include the electric field in our formulation in a future work.

ACKNOWLEDGMENTS

This work was supported by Taiwan National Science Council under Contract No. NSC82-0208-M006-020.

- ¹A. Zrenner, P. Leeb, J. Schäfer, G. Böhm, G. Weimann, J. M. Worlock, L. T. Florez, and J. P. Harbison, *Surf. Sci.* **263**, 496 (1992).
- ²J. Feldmann, M. Preis, E. O. Göbel, P. Dawson, C. T. Foxon, and I. Galbraith, *Solid State Commun.* **83**, 245 (1992).
- ³A. Ishibashi, Y. Mori, M. Itahashi, and N. Watanabe, *J. Appl. Phys.* **58**, 2691 (1985).
- ⁴M. D. Sturge, E. Finkman, and M. C. Tamargo, *J. Lumin.* **40**, 425 (1988).
- ⁵T. Isu, D.-S. Jiang, and K. Ploog, *Appl. Phys. A* **43**, 75 (1987).
- ⁶B. A. Wilson, C. E. Bonner, R. C. Spitzer, P. Dawson, K. J. Moore, and C. T. Foxon, *J. Vac. Sci. Technol. B* **6**, 1156 (1988).
- ⁷J. Feldmann, R. Sattmann, E. O. Göbel, J. Kuhl, J. Hebling, K. Ploog, R. Muralidharan, P. Dawson, and C. T. Foxon, *Phys. Rev. Lett.* **62**, 1892 (1989).
- ⁸M. Dutta, D. D. Smith, P. G. Newman, X. C. Liu, and A. Petrou, *Phys. Rev. B* **42**, 1474 (1990).
- ⁹I. L. Aleiner, E. L. Ivchenko, V. P. Kochereshko, G. L. Sandler, P. Lavallard, and R. Planel, *Superlatt. Microstruct.* **13**, 237 (1993).
- ¹⁰G. Danna, F. R. Ladan, F. Mollot, and R. Planal, *Appl. Phys. Lett.* **51**, 1605 (1987).
- ¹¹M.-H. Meynadier, R. E. Nahory, J. M. Worlock, M. C. Tamargo, J. L. de Miguel, and M. D. Sturge, *Phys. Rev. Lett.* **60**, 1388 (1988).
- ¹²M. Dutta, H. Shen, D. D. Smith, K. K. Chio, and P. G. Newman, *Surf. Sci.* **267**, 474 (1992).
- ¹³M. J. Gell, D. Ninno, M. Jaros, D. J. Wolford, T. F. Keuch, and J. A. Bradley, *Phys. Rev. B* **35**, 1196 (1987).
- ¹⁴M. S. Sholnick, G. W. Smith, I. L. Spain, C. R. Whitehouse, D. C. Herbert, D. M. Whittaker, and L. J. Reed, *Phys. Rev. B* **39**, 11 191 (1989).
- ¹⁵J. H. Burnett, H. M. Cheong, W. Paul, E. S. Koteles, and B. Elman, *Phys. Rev. B* **47**, 1991 (1993).
- ¹⁶Yan-Ten Lu and L. J. Sham, *Phys. Rev. B* **40**, 5567 (1989).
- ¹⁷J. N. Schulman and T. C. McGill, *Phys. Rev. Lett.* **39**, 1681 (1977).
- ¹⁸D. Z.-Y. Ting and Y.-C. Chang, *Phys. Rev. B* **36**, 4359 (1987).
- ¹⁹I. P. Batar, S. Ciraci, and J. S. Nelson, *J. Vac. Sci. Technol. B* **5**, 1300 (1987).
- ²⁰M. A. Gell and D. C. Herbert, *Phys. Rev. B* **35**, 9591 (1987).
- ²¹S.-H. Wei and A. Zunger, *J. Appl. Phys.* **63**, 5795 (1988).
- ²²S. Massidda, B. I. Min, and A. J. Freeman, *Phys. Rev. B* **38**, 1970 (1988).
- ²³S. Gopalan, N. E. Christensen, and M. Cardona, *Phys. Rev. B* **39**, 5165 (1989).
- ²⁴T. Ando and H. Akera, *Phys. Rev. B* **40**, 11 619 (1989).
- ²⁵N. J. Pulsford, R. J. Nicholas, P. Dawson, K. J. Moore, G. Duggan, and C. T. B. Foxon, *Phys. Rev. Lett.* **63**, 2284 (1989).
- ²⁶I. Morrison, L. D. L. Brown, and M. Jaros, *Phys. Rev. B* **42**, 11 818 (1990).
- ²⁷Y. Fu, M. Willander, E. L. Ivchenko, and A. A. Kiselev, *Phys. Rev. B* **47**, 13 498 (1993).
- ²⁸D. A. Broido and L. J. Sham, *Phys. Rev. B* **34**, 3917 (1986).
- ²⁹G. D. Sanders and Y. C. Chang, *Phys. Rev. B* **35**, 1300 (1987).
- ³⁰G. Duggan and H. I. Ralph, *Phys. Rev. B* **35**, 4152 (1987).
- ³¹M. M. Dignam and J. E. Sipe, *Phys. Rev. B* **41**, 2865 (1990).

- ³²J. Cen and K. K. Bajaj, Phys. Rev. B **45**, 14 380 (1992).
- ³³R. Zimmermann and D. Bimberg, Phys. Rev. B **47**, 15 789 (1993).
- ³⁴J.-W. Wu, Phys. Rev. B **40**, 8490 (1989).
- ³⁵S. L. Chuang, S. Schmitt-Rink, D. A. B. Miller, and D. S. Chemla, Phys. Rev. B **43**, 1500 (1991).
- ³⁶C. Y-P Chao and S. L. Chuang, Phys. Rev. B **43**, 6530 (1991).
- ³⁷H. C. Liu, Appl. Phys. Lett. **51**, 1019 (1987).
- ³⁸D. B. Tran Thoai, R. Zimmermann, M. Grundmann, and D. Bimberg, Phys. Rev. B **42**, 5906 (1990).
- ³⁹L. Wendler and B. Hartwig, J. Phys. Condens. Matter **3**, 9907 (1991).
- ⁴⁰U. Fano, Phys. Rev. **124**, 1866 (1961).